Rational design of a targeted theranostic nanoagent for sequential application during oral squamous cell carcinoma surgery

Danni Shan[1*], Diya Xie[1*], Liping Zeng[1], Jianquan Wang[2*] and Zhiyong Wang[1*]

D. Shan, D. Xie, L. Zeng, J. Wang, Z. Wang

[1]Nanjing Stomatological Hospital, Affiliated Hospital of Medical School, Institute of Stomatology, Nanjing University, Nanjing 210008, China.

[2]College of Materials Engineering, Jinling Institute of Technology, Nanjing 211169, China.

Danni Shan[1*]

Diya Xie[1*]

*These authors contributed equally to this work

*Corresponding authors:

Zhiyong Wang

E-mail：zywangkq@nju.edu.cn

Jianquan Wang

E-mail：wangjianquan006@163.com

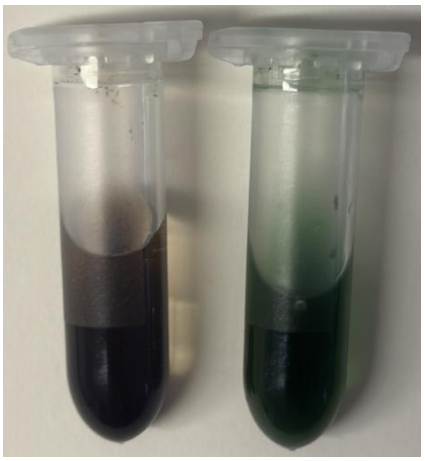

Supplementary Fig. 1 Photographs of AuNPs (left) and AuNPs/HSA-ICG solution（right).

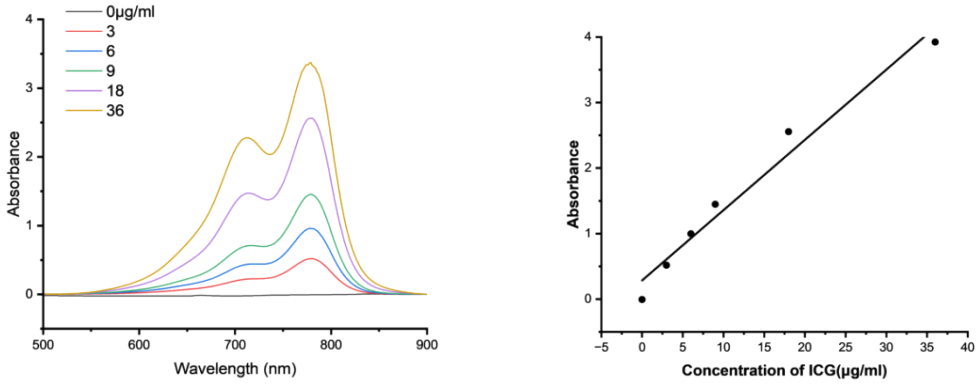

Supplementary Fig. 2 Determination of ICG concentration in AuNPs/HSA-ICG. **A** Absorbance of different concentrations of ICG. **B** A standard curve based on Figure A.

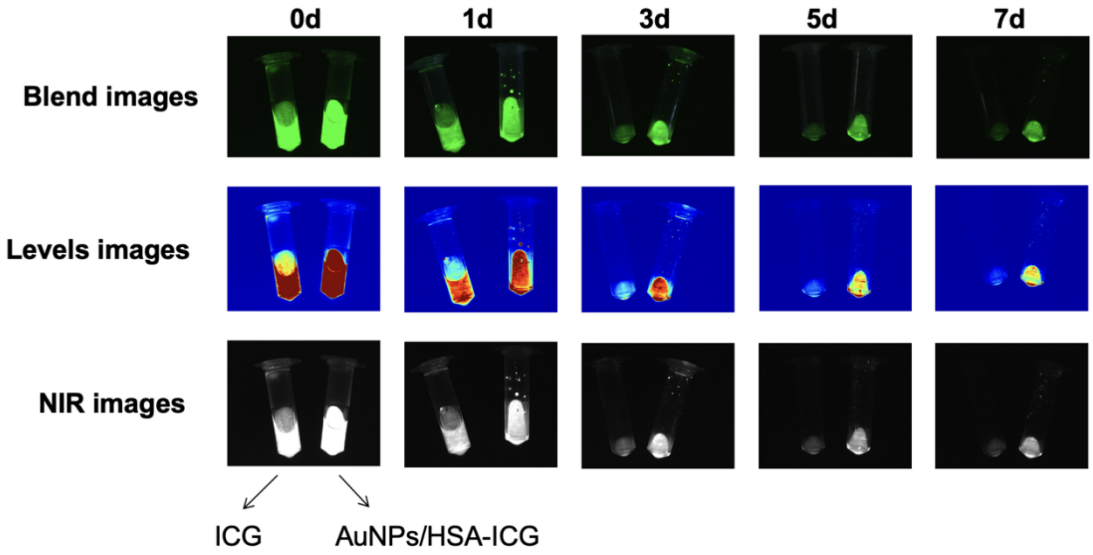

Supplementary Fig. 3 Fluorescence intensity change images of ICG (left) and AuNPs/HSA-ICG (right) within 7 d.

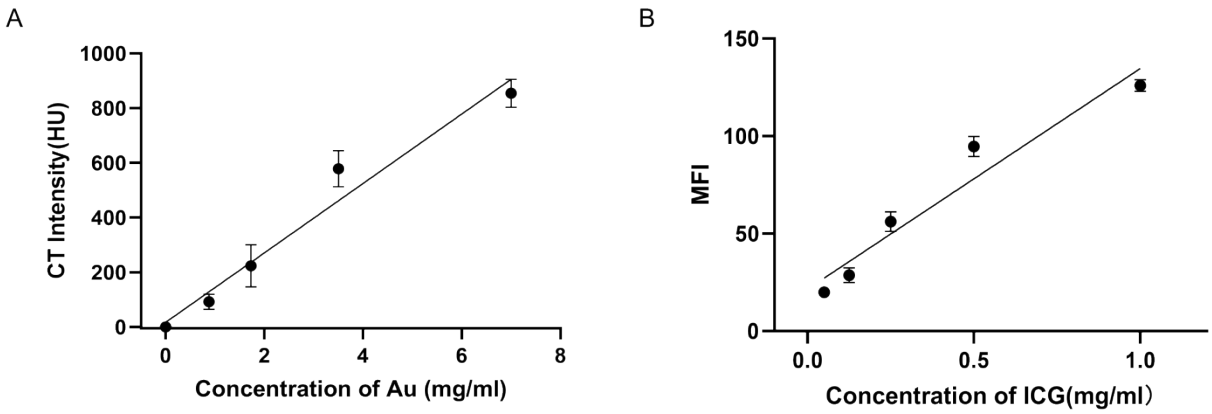

Supplementary Fig. 4 A Hounsfield unit (HU) values for different concentrations of AuNPs/HSA-ICG. **B** MFI for different concentrations of AuNPs/HSA-ICG.

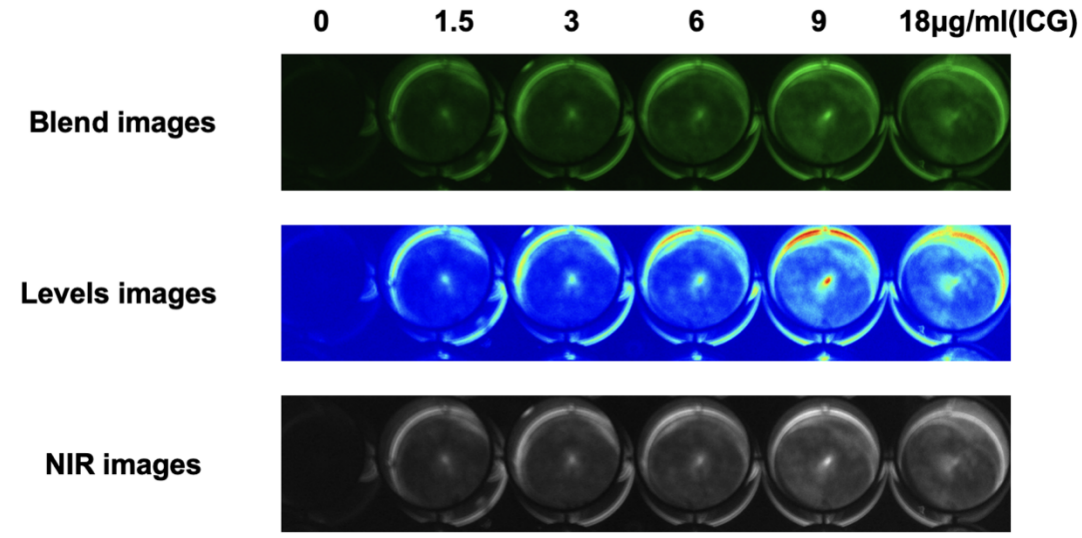

Supplementary Fig. 5 The FI images of cellular uptake, as the concentration of AuNPs/HSA-ICG increases.

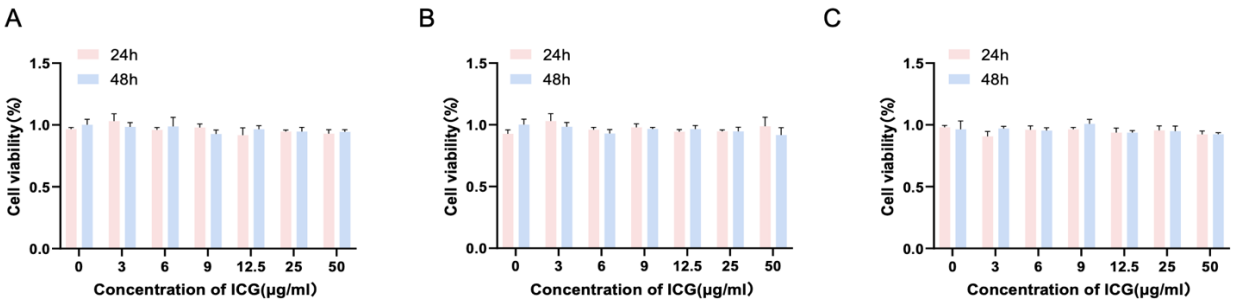

Supplementary Fig. 6 Cytoviability of HUVEC (left), SCC7(middle), HSC3(right)cells after incubation with the NPs for 24 and 48 h, respectively.

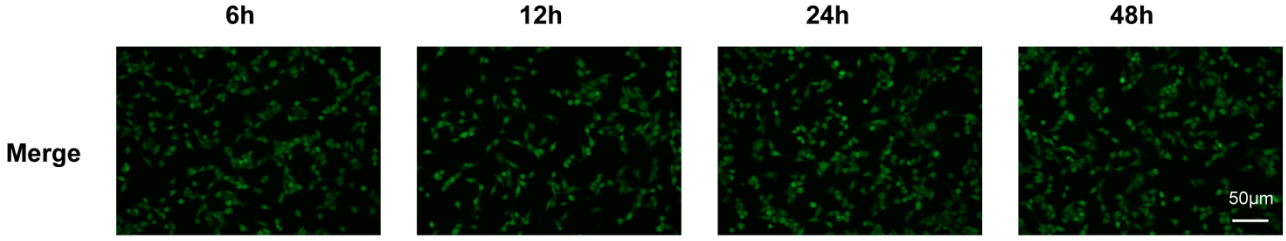

Supplementary Fig. 7 The inverted fluorescence micrographs of live/dead staining.

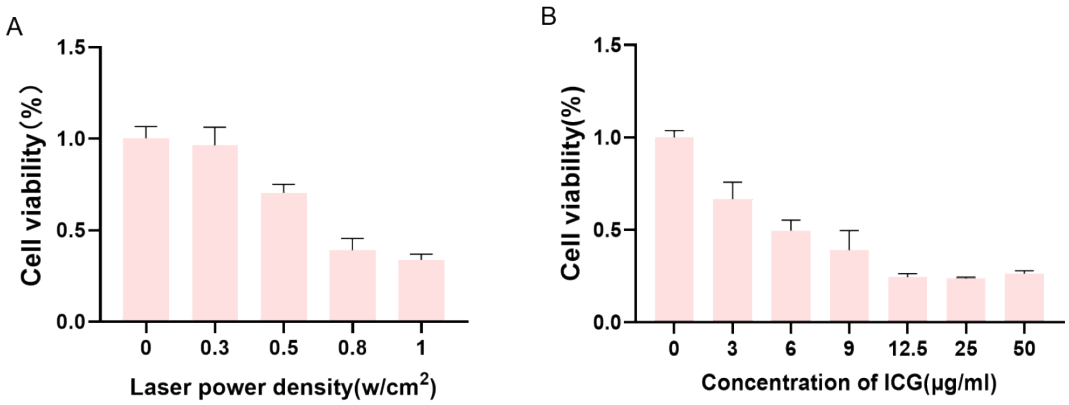

Supplementary Fig. 8 Changes in cell viability under different laser irradiation powers(A) and different concentration (B).

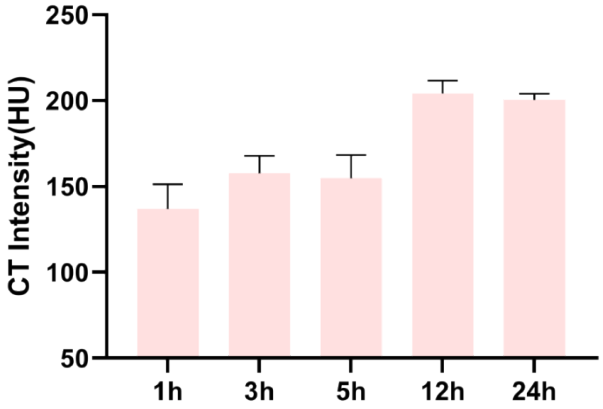

Supplementary Fig. 9 Quantitative analysis of in vivo CT imaging.

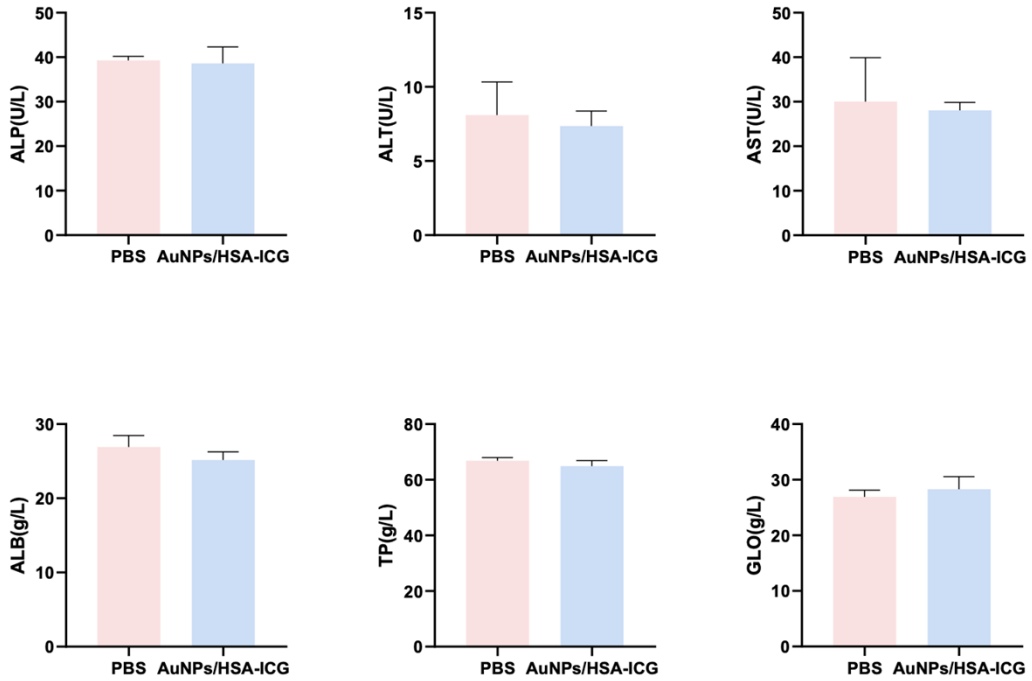

Supplementary Fig. 10 Main liver function indicators of healthy mice.

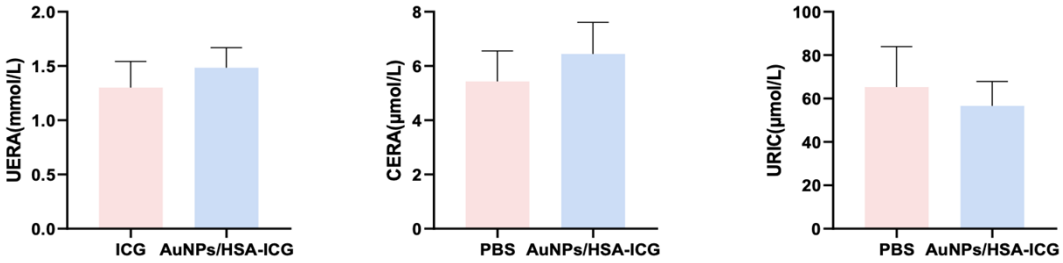

Supplementary Fig. 11 Main renal functions indexes of healthy mice.

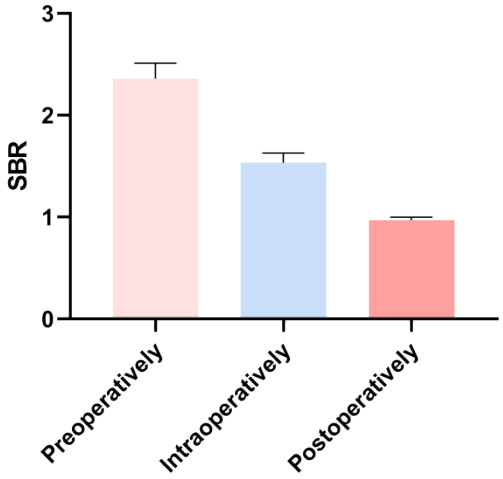

Supplementary Fig. 12 Quantitative SBR analysis of fluorescence-guided tumor resection

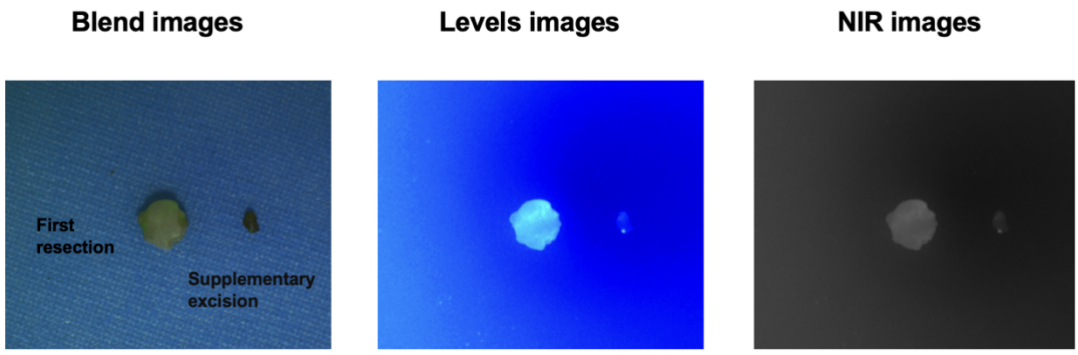

Supplementary Fig. 13 Tissue excised during Image-guided surgery.

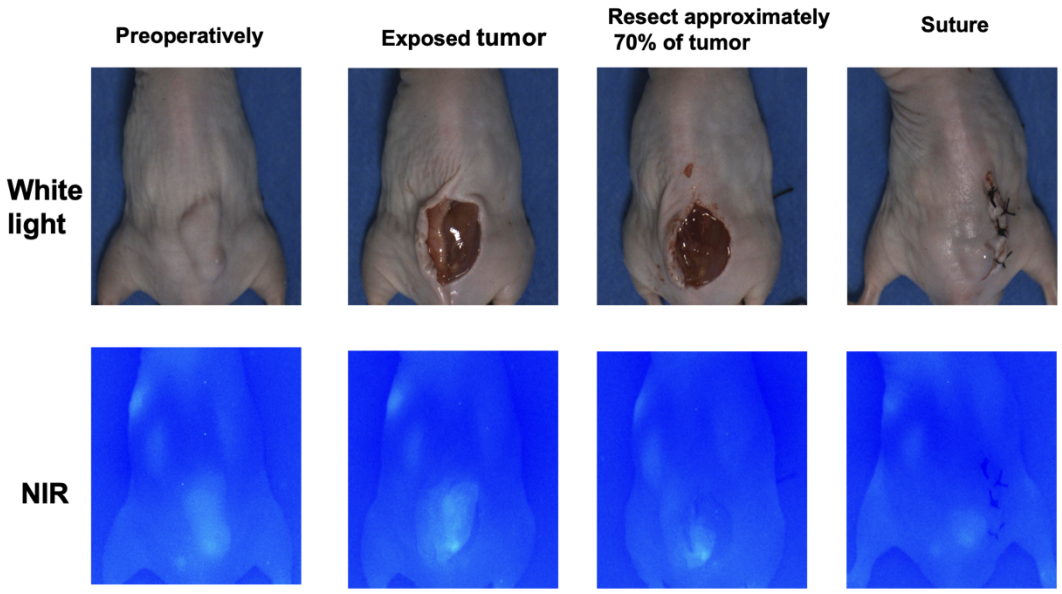

Supplementary Fig. 14 Construction process of residual tumor models.

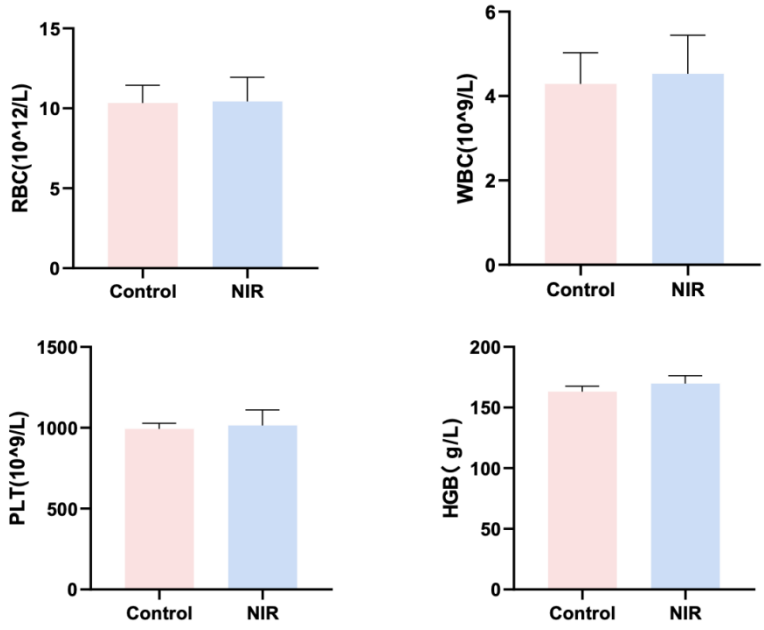

Supplementary Fig. 15 Main hematological data of mice after PDT.

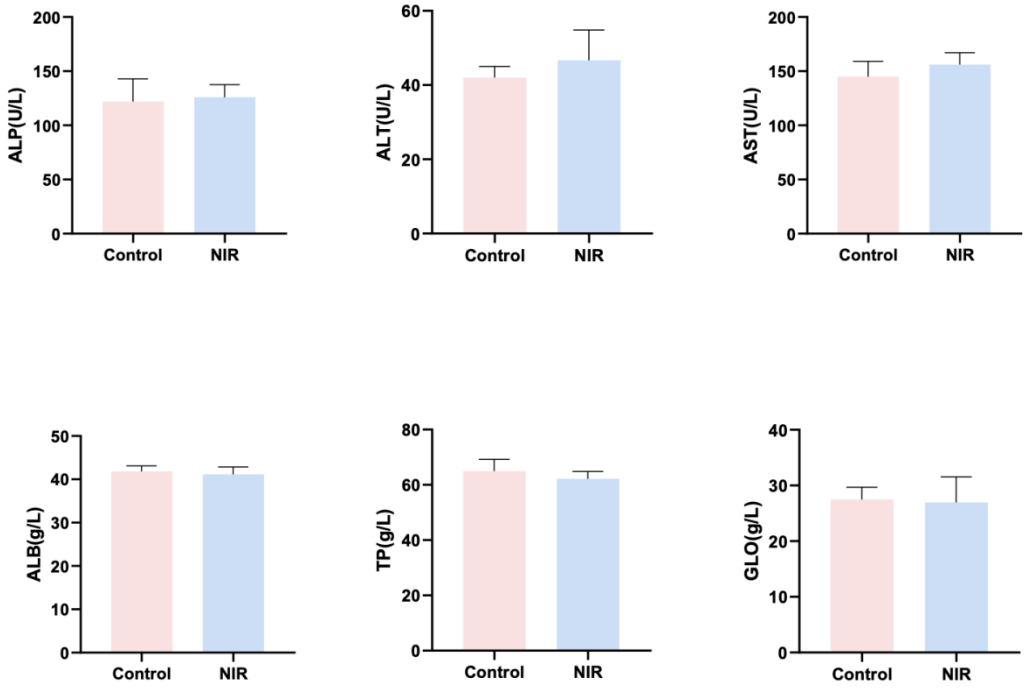

Supplementary Fig. 16 The major liver functions indexes of mice after PDT.

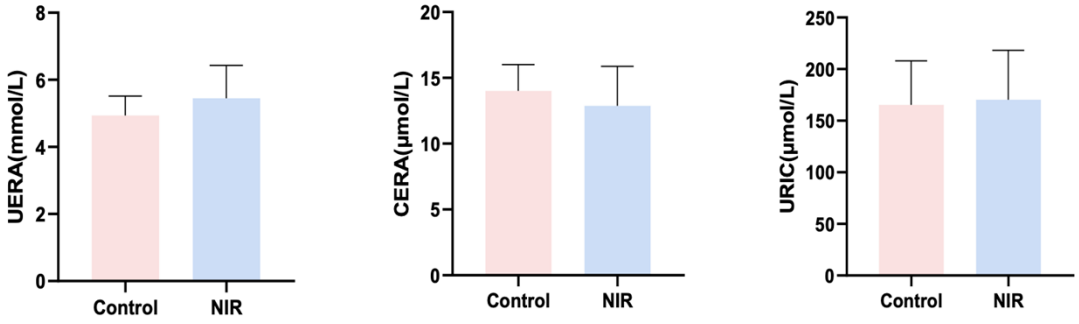

Supplementary Fig. 17 The major renal functions indexes of mice after PDT.

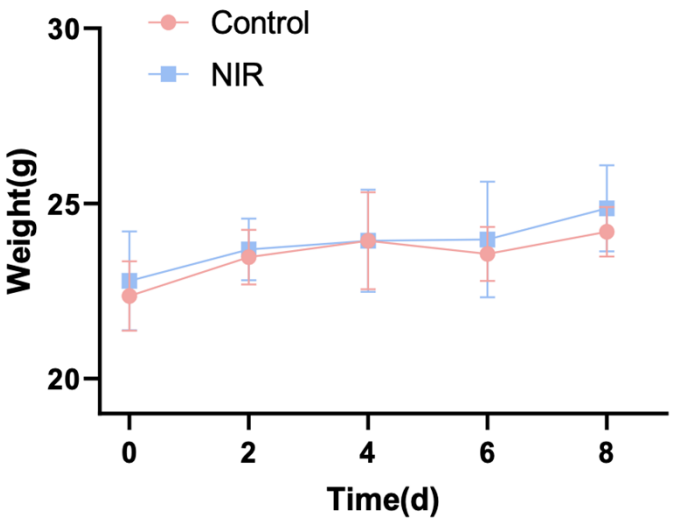

Supplementary Fig. 18 Changes in mice body weight during PDT.